

**Normal Mode Energetics of the General  
Circulation during the FGGE Winter**

**BY**

**H.L. TANAKA**

*Reprinted from the Science Reports of  
the Institute of Geoscience, University of Tsukuba  
Section A, Volume 15, pp. 1-19  
January 25, 1994*

---



## Normal Mode Energetics of the General Circulation during the FGGE Winter

BY

H.L. TANAKA

### Contents

1. Introduction .....	1
2. Data .....	3
3. Scheme of Analysis .....	3
4. Energy Distributions .....	7
5. Energy Interactions .....	13
6. Summary and Conclusions .....	17
Acknowledgments .....	17
References .....	17
Appendix .....	19

### Abstract

A diagnostic energetics scheme is developed in order to investigate the energy flows in the three-dimensional spectral domain (Hough modes in horizontal) in the atmosphere. This energetics scheme is applied to the GFDL version of the FGGE level IIIb data during the winter from December 1978 to February 1979.

The resultant energy flow of the general circulation is summarized as follows: Atmospheric energy is generated at zonal baroclinic components, especially at the vertical mode  $m=4$ . The generated zonal energy at the baroclinic components (referred to as baroclinic energy) is first converted to eddy baroclinic energy, then to eddy energy at the barotropic component (referred to as barotropic energy). Accumulated eddy barotropic energy at the synoptic-scale disturbances is finally transformed to zonal barotropic energy by the process of up-scale energy cascade. Hence, atmospheric jet stream is accelerated by eddies so that the jet structure becomes more barotropic in the vertical.

Parameterizing the horizontal scale of waves by their eigenfrequencies of the Hough modes, we find that the energy spectrum of the synoptic-scale Rossby modes obeys approximately the 3 power of the eigenfrequency, as expected from the 2-dimensional turbulent theory. However, for the largest-scale Rossby modes in the planetary waves, the spectrum obeys the  $-5/3$  power law and merges with the spectrum of the largest-scale gravity modes. It is concluded from the results that the energy spectrum of the global circulation has both 3 and  $-5/3$  power regimes within the barotropic planetary waves.

### 1. Introduction

Since the atmospheric energy flow was discussed by Lorenz (1955) using the concept of available potential energy, the energetical

role of the atmospheric eddies has been extensively investigated. Saltzman (1957) expanded the energy equations into the wavenumber domain and showed that the

kinetic energy of the cyclone-scale waves is transformed into both the planetary waves and the short waves in terms of nonlinear wave-wave interactions. The study by Saltzman was followed by Kao (1968) and Hayashi (1980) who extended this approach to the wavenumber-frequency domain making use of the two-dimensional Fourier expansion or the space-time spectral method. The energy decomposition was further pursued in the meridional wavenumber domain using spherical harmonics (Eliassen and Machenhauer, 1965) and in the vertical wavenumber domain using empirical orthogonal functions (Holmström, 1963).

Kasahara (1976), on the other hand, showed a computational scheme of Hough functions (called horizontal normal mode functions) in the barotropic atmosphere. The Hough functions are the eigensolution of linearized primitive equations over a sphere and have been applied extensively to nonlinear normal mode initialization techniques. He applied the Hough functions to an orthonormal basis for the energy decomposition in the meridional wavenumber domain. Since Kasahara and Puri (1981) first obtained orthonormal eigensolutions to the vertical structure equation, it became possible to expand the atmospheric data into the three-dimensional harmonics of the eigen-solutions. The normal mode approach is useful especially for the research of tropical waves because Kelvin waves or mixed Rossby-gravity waves are obtained as the normal modes in the atmospheric oscillations. Recently, some oscillation in the middle latitude atmosphere, such as 5-day waves or 16-day waves, are identified with external Rossby waves of (1,1) and (1,3) modes, respectively (see Madden, 1978). According to Lindzen et al. (1984), the observed planetary scale oscillation are identified with the low-order external Rossby waves which are expected by the theoretical research. They compared two versions of the

FGGE data by the European Center for Medium Range Weather Forecast and the Goddard Laboratory for Atmospheric Science, and verified that the waves are not the artificial products by the General Circulation Models but the characteristics of the observed atmosphere.

It is still uncertain, however, how these modes are created, amplified or dissipated. This problem is closely related with an amplification of planetary waves in conjunction with the blocking phenomena in the troposphere and the sudden warming in the stratosphere. Garcia and Geisler (1981) suggested that the waves are created by stochastic noise. Regularly oscillating zonal wind (Hirota, 1971) may be one of the explanations for the variations of the atmospheric normal mode. Although several researchers investigated the statistics (Kasahara, 1976) or time variations (Lindzen et al., 1984) of the normal modes by projecting the energy onto the Hough functions, the energy flow among these modes has not been investigated in the previous research so far.

In this paper we have developed a diagnostic energetics scheme which describes the energy flow among the different modes in the atmosphere. Hereafter, we will call such a scheme a normal mode energetics scheme in reference to the spectral energetics scheme by Saltzman. In order to develop the normal mode energetics scheme, we have applied the technique of the three-dimensional expansion into normal mode functions developed by Kasahara and Puri (1981). This scheme can provide much information concerning the energetics for particular normal modes such as 5-day waves or 16-day waves. By summing the normal mode energetic terms within the same physical categories, for example, barotropic mode, baroclinic mode, Rossby mode or gravity mode, it is also possible to investigate the energy interactions among them. By applying the normal mode energetics scheme

to a data set of the First GARP (Global Atmospheric Research Program) Global Experiment (FGGE) by the Geophysical Fluid Dynamics Laboratory (GFDL), we investigated the energy distributions and the energy interactions as functions of zonal wavenumber, vertical wavenumber and meridional wavenumber. Since each normal mode is associated with one eigenfrequency, it is also attempted to present the energy distributions in the eigenfrequency domain.

## 2. Data

The GFDL version of the FGGE IIIb data for 1 December 1978 though 30 November 1979 were obtained from the World Data Center A for Meteorology at Asheville, North Carolina, U.S.A. The FGGE data on a  $1.875^\circ \times 1.875^\circ$  latitude-longitude grid were interpolated to a  $4^\circ \times 5^\circ$  grid with 46 latitudes from  $90^\circ$  S to  $90^\circ$  N and 72 longitudes from  $0^\circ$  to  $355^\circ$  E. The twice daily (0000 and 1200 GMT) meteorological variables of horizontal wind, vertical p-velocity, temperature and geopotential height are defined at 12 vertical levels of 1000, 850, 700, 500, 400, 300, 250, 200, 150, 100, 50, 30 hPa. These FGGE data are the same as used by Kung and Tanaka (1983, 1984) for the spectral energetics analysis of the global circulation (refer to these papers for details). The winter three months from December 1978 to February 1979 are analyzed although the vertical eigenfunctions and the Hough vector functions are computed based on the annual mean global mean temperature.

The GFDL version is selected from several versions of the FGGE data because a global optimum interpolation analysis in the final stage of 4-dimensional assimilation process (Miyakoda et al., 1982) seems to enhance the quality of data as the observed atmosphere. The gravity wave component should be retained as well as the Rossby waves even though the statistical interpolation process tends to lose the dynamical consistency of the

data.

## 3. Scheme of Analysis

A normal mode in a realistic mean zonal wind has not been obtained so far. It is discussed by Kasahara (1980) and Salby (1981) that the Hough functions in a motionless atmosphere would be distorted by the presence of the realistic basic state. As is pointed out by Ahlquist (1982), however, the distortion is small for the lowest-order Hough modes. In this study, the atmospheric data have been projected onto the Hough functions obtained for motionless atmosphere as in Kasahara (1976) or Lindzen et al. (1984).

A set of primitive equations with p-coordinate in the vertical may be written as

$$\begin{aligned} \frac{\partial u}{\partial t} - 2\Omega \sin\theta v + \frac{1}{a \cos\theta} \frac{\partial \phi}{\partial \lambda} \\ = -V \cdot \nabla u - \omega \frac{\partial u}{\partial p} + \frac{\tan\theta}{a} uv + F_u, \end{aligned} \quad (1)$$

$$\begin{aligned} \frac{\partial v}{\partial t} + 2\Omega \sin\theta u + \frac{1}{a} \frac{\partial \phi}{\partial \theta} \\ = -V \cdot \nabla v - \omega \frac{\partial v}{\partial p} - \frac{\tan\theta}{a} uv + F_v, \end{aligned} \quad (2)$$

$$\begin{aligned} \frac{\partial}{\partial t} \left[ - \left( \frac{\partial}{\partial p} \frac{p^2}{R\gamma} \frac{\partial}{\partial p} \right) \phi \right] + \nabla \cdot V \\ = \frac{\partial}{\partial p} \left[ \frac{p}{\gamma} (-V \cdot \nabla T - \omega \frac{\partial T}{\partial p}) \right] \\ + \frac{\partial}{\partial p} \frac{pQ}{cp} \gamma, \end{aligned} \quad (3)$$

where

$$\gamma = \frac{RT_0}{C_p} - p \frac{dT_0}{dp}. \quad (4)$$

The symbols used in the equations are customary and summarized in the Appendix. In order to obtain the energy conservation law, one term has been neglected in (3) assuming that the perturbation temperature,  $T$ , is negligible compared with the basic state temperature,  $T_0$  (see Holton, 1975). The stability parameter,  $\gamma$ , which is determined by the basic state temperature is a function of  $p$

only. The right hand sides of (1)-(3) involve nonlinear terms, frictional forces and a diabatic heat source.

By a separation of variables for the linearized version of (1)-(3), we obtain a vertical structure equation which constitutes an eigenvalue problem to obtain equivalent heights,  $h_m$ ,

$$\left(\frac{d}{dp} \frac{p^2}{R\gamma} \frac{d}{dp}\right) G_m(p) + \frac{1}{gh_m} G_m(p) = 0. \quad (5)$$

Applied to the proper boundary conditions, Eq. (5) is solved by a finite difference method. The  $m$ -th vertical eigenvectors,  $G_m(p)$ , satisfy the orthonormal condition:

$$\frac{1}{p_s} \int_0^{p_s} G_m(p) G_j(p) dp = \delta_{mj}, \quad (6)$$

where the subscript  $j$  refers to a different eigenvector, and  $\delta_{mj}$  denotes Kronecker delta. Global mean surface pressure,  $p_s$ , is substituted for (6). Refer to Kasahara and Puri (1981) and Kasahara (1984) for discrete and continuous formula to get a set of orthonormal eigenvectors. The basic state temperature,  $T_0$ , stability parameter,  $\gamma$ , and equivalent height,  $h_m$ , are listed in Table 1. Global mean temperature of the FGGE data is averaged for one year from December 1978 through November 1979 to obtain  $T_0$ .

Fig. 1 illustrates the orthonormal vertical eigenvectors obtained by the finite difference scheme with 12 vertical levels. The vertical mode  $m = 0$  is called a barotropic mode because the values of the mode are approximately constant and have no node in the vertical. The vertical mode  $m = 1$  has one node in the vertical,  $m = 2$  has two nodes and so on. The vertical mode number is defined in this paper so that the mode number corresponds to the number of nodes in the vertical. The modes  $m > 1$  are regarded as baroclinic modes. The vertical structure for the higher modes may depend on the selection of vertical levels for finite difference method.

Table 1. Global mean temperature  $T_0$ , stability parameter  $\gamma$ , and equivalent height  $h_m$ .

$P$ (mb)	$T_0$ (K)	$\gamma$ (K)	$m$	$h_m$ (m)
30	215.56	66.84	0	9623.9
50	212.72	67.91	1	2297.1
100	205.49	57.62	2	475.9
150	211.44	39.55	3	272.0
200	219.17	33.77	4	150.0
250	225.94	28.65	5	79.5
300	233.47	22.51	6	42.4
400	247.63	20.23	7	26.3
500	258.97	24.19	8	21.6
700	274.38	34.36	9	13.4
850	282.48	37.07	10	9.4
1000	289.82	33.84	11	9.0

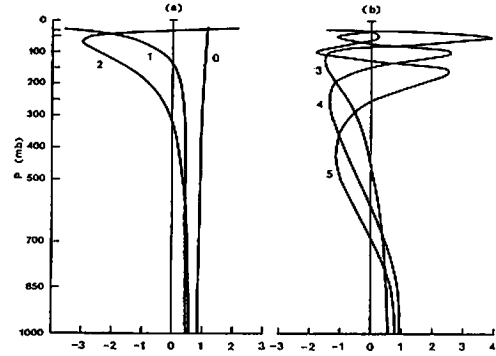


Fig. 1. Vertical eigenvectors for (a) vertical modes  $m=0-2$ , and (b)  $m=3-5$ .

Using the orthonormal condition (6), we can construct a set of vertical transforms:

$$f(p) = \sum_{m=0}^{\infty} f_m G_m(p), \quad (7)$$

$$f_m = \frac{1}{p_s} \int_0^{p_s} f(p) G_m(p) dp, \quad (8)$$

where  $f(p)$  is an arbitrary function of pressure. By applying the vertical transforms to (1)-(3), we obtain a dimensionless equation in a vector form:

$$\frac{\partial}{\partial t} W_m + L W_m = B_m + C_m + D_m, \quad (9)$$

where

$$W_m = \begin{pmatrix} u_m \\ v_m \\ \phi_m \end{pmatrix} = \begin{pmatrix} (gh_m)^{1/2} & 0 & 0 \\ 0 & (gh_m)^{1/2} & 0 \\ 0 & 0 & gh_m \end{pmatrix}^{-1} \begin{pmatrix} u \\ v \\ \phi \end{pmatrix} \quad (10)$$

$$B_m = \begin{pmatrix} 2\Omega(gh_m)^{1/2} & 0 & 0 \\ 0 & 2\Omega(gh_m)^{1/2} & 0 \\ 0 & 0 & 2\Omega \end{pmatrix}^{-1} = \begin{pmatrix} -V \cdot \nabla u - \omega \frac{\partial u}{\partial p} - \frac{\tan \theta}{a} uv \\ -V \cdot \nabla v - \omega \frac{\partial v}{\partial p} - \frac{\tan \theta}{a} uv \\ 0 \end{pmatrix} \quad (11)$$

$$C_m = \begin{pmatrix} 2\Omega(gh_m)^{1/2} & 0 & 0 \\ 0 & 2\Omega(gh_m)^{1/2} & 0 \\ 0 & 0 & 2\Omega \end{pmatrix}^{-1} = \begin{pmatrix} 0 \\ 0 \\ \frac{\partial}{\partial p} \left( \frac{p}{\gamma} [-V \cdot \nabla T - \omega \frac{\partial T}{\partial p}] \right) \end{pmatrix} \quad (12)$$

$$D_m = \begin{pmatrix} 2\Omega(gh_m)^{1/2} & 0 & 0 \\ 0 & 2\Omega(gh_m)^{1/2} & 0 \\ 0 & 0 & 2\Omega \end{pmatrix}^{-1} = \begin{pmatrix} F_u \\ F_v \\ \frac{\partial}{\partial p} \left( \frac{pQ}{c_p \gamma} \right) \end{pmatrix} \quad (13)$$

The subscript  $m$  denotes the  $m$ -th component of the vertical transform. After obtaining the  $m$ -th vertical component, we make the vectors dimensionless by a scaling matrix involving the equivalent height  $h_m$  and  $2\Omega$  for time. The linear operator,  $L$ , is given by

$$L = \begin{pmatrix} 0 & -\sin \theta & \alpha_m \frac{\partial}{\cos \theta} \\ \sin \theta & 0 & \alpha_m \frac{\partial}{\partial \theta} \\ \frac{\alpha_m}{\cos \theta} \frac{\partial}{\partial \lambda} & \frac{\alpha_m}{\cos \theta} \frac{\partial}{\partial \theta} \cos \theta & 0 \end{pmatrix} \quad (14)$$

where the dimensionless coefficient,  $\alpha_m$ , is defined as

$$\alpha_m = \frac{(gh_m)^{1/2}}{2\Omega a} \quad (15)$$

The linearized equation (9) substituted by zero for the right hand side is called a horizontal structure equation (Laplace's tidal equation), and the solutions are called Hough harmonics,  $H_{srm}$ . The Hough harmonics are obtained as an eigenvalue problem with eigenfrequencies for the free waves:

$$-i\sigma_{srm}H_{srm} + LH_{srm} = 0, \quad (16)$$

where

$$H_{srm}(\lambda, \theta) = \theta_{srm}(\theta) \exp(is\lambda), \quad (17)$$

and the Hough vector functions,  $\theta_{srm}$ , are given by

$$\theta_{srm} = \begin{pmatrix} U \\ -iV \\ Z \end{pmatrix}_{srm}(\theta). \quad (18)$$

Refer to Longuet-Higgins (1968) and Kasahara (1976) for details concerning the Hough vector functions. The subscripts  $s$  and  $r$  denote zonal wavenumber and meridional mode number, respectively. The meridional mode number is defined as a sequence of the three distinct modes. The one is a westward propagating Rossby mode specified by  $l_R$ . The other two are westward and eastward propagating gravity modes,  $l_W$  and  $l_E$ . The Hough harmonics satisfy the orthonormal condition in the following sense:

$$\frac{1}{2\pi} \int_{-\pi/2}^{\pi/2} \int_0^{2\pi} H_{srm}^* \cdot H_{s'r'm'} \cos \theta d\lambda d\theta = \delta_{ss'} \delta_{rr'} \quad (19)$$

where the asterisk denotes a complex conjugate and the primes refer to another Hough harmonics.

Using the orthonormal condition, we can construct a set of Fourier-Hough transforms:

$$W_m(\lambda, \theta, t) = \sum_{s=-\infty}^{\infty} \sum_{r=0}^{\infty} w_{srm}(t) H_{srm}(\lambda, \theta). \quad (20)$$

$$w_{srm}(t) = \frac{1}{2\pi} \int_{-\pi/2}^{\pi/2} \int_0^{2\pi} H_{srm}^* \cdot W_m \cos\theta d\lambda d\theta. \quad (21)$$

By applying the Fourier-Hough transforms to (9), we obtain

$$\frac{d}{dt} w_{srm} + i\sigma_{srm} w_{srm} = b_{srm} + c_{srm} + d_{srm}, \quad (22)$$

where the complex variables  $w_{srm}$ ,  $b_{srm}$ ,  $c_{srm}$ , and  $d_{srm}$  are the Fourier-Hough transforms of the vectors of (10)-(13), respectively. According to (22), the time change of the complex expansion coefficient of a normal mode,  $w_{srm}$ , is caused by four terms, i.e., a linear term related with phase change of the wave, nonlinear terms due to wind field and mass field, and a diabatic process. Since the eigenfrequency  $\sigma_{srm}$  is always real, the linear term contributes only to the phase change of the wave, but not to the amplitude change.

On the other hand, the summation of kinetic energy,  $K$ , and available potential energy,  $A$ , is conserved provided that  $F_u = F_v = 0$  and  $Q = 0$  (see Kasahara and Puri, 1981):

$$\frac{d}{dt} \left[ \frac{1}{gS} \int_S^{p_s} E dp + \frac{1}{2} \frac{p_s}{RT_s} \phi_s^2 dS \right] = 0, \quad (23)$$

where

$$E = K + A, \quad (24)$$

$$K = \frac{1}{2} (u^2 + v^2), \quad (25)$$

$$A = \frac{1}{2} \frac{p^2}{R\gamma} \left( \frac{\partial\phi}{\partial p} \right)^2, \quad (26)$$

and the subscripts  $s$  for the coefficients denote surface value of the basic state here. By expanding the dependent variables in (23) into the vertical normal modes using (7), the equation of energy conservation is reduced to a sum of squares of dimensionless variables  $u_m$ ,  $v_m$ , and  $\phi_m$ :

$$\frac{d}{dt} \left[ \sum_{m=0}^{\infty} \frac{p_s h_m}{2S} \int_S (u_m^2 + v_m^2 + \phi_m^2) dS \right] = 0. \quad (27)$$

Moreover, by expanding them into the Hough harmonics using (20), we finally obtain the equation of energy conservation in terms of a summation of energies associated with each mode:

$$\sum_{m=0}^{\infty} \sum_{l=0}^{\infty} \sum_{z=0}^{\infty} \frac{d}{dt} E_{srm} = 0, \quad (28)$$

where

$$E_{0rm} = \frac{1}{4} p_s h_m |w_{0rm}|^2, \quad (29)$$

$$E_{srm} = \frac{1}{2} p_s h_m |w_{srm}|^2. \quad (30)$$

The energy of a normal mode is defined as the square of the absolute value of the complex expansion coefficient, multiplied by a dimensional factor chosen so that the energy is expressed in  $\text{Jm}^{-2}$ . The kinetic energy of zonal and meridional components,  $K_u$  and  $K_v$ , and the available potential energy,  $A$ , for each mode, may be approximated by  $E_{srm}$  through multiplication by coefficients,  $\beta_u$ ,  $\beta_v$ ,  $\beta_z$  which represent energy ratios of  $U$ ,  $V$ , and  $Z$  of the normalized Hough vector functions:

$$\begin{aligned} \begin{pmatrix} K_u \\ K_v \\ A \end{pmatrix}_{srm} &= E_{srm} \begin{pmatrix} \beta_u \\ \beta_v \\ \beta_z \end{pmatrix}_{srm} \\ &= E_{srm} \int_{-\pi/2}^{\pi/2} \begin{pmatrix} U^2 \\ V^2 \\ Z^2 \end{pmatrix}_{srm} \cos\theta d\theta. \end{aligned} \quad (31)$$

In general, this separation of energy is not correct because  $U$ ,  $V$ ,  $Z$  are not orthogonal to one another. However, the energy separation in  $K$  and  $A$  so obtained is comparable to the physical separation by the established spectral energetics by Saltzman. This fact suggests that the present energy separation is a good approximation to the reality.

In order to obtain energy balance equations for the normal modes, Eqs. (29) and (30) are differentiated with respect to time,  $t$ . Substituting (22) into the time derivatives of



$w_{srm}$ , we obtain finally:

$$\frac{d}{dt} E_{srm} = B_{srm} + C_{srm} + D_{srm}, \quad (32)$$

where

$$B_{srm} = \rho_s \Omega h_m [w_{srm}^* b_{srm} + w_{srm} b_{srm}^*], \quad (33)$$

$$C_{srm} = \rho_s \Omega h_m [w_{srm}^* c_{srm} + w_{srm} c_{srm}^*], \quad (34)$$

$$D_{srm} = \rho_s \Omega h_m [w_{srm}^* d_{srm} + w_{srm} d_{srm}^*]. \quad (35)$$

According to (32), the time change of  $E_{srm}$  is caused by the three terms which appear in the right hand side of (32). The terms  $B_{srm}$  and  $C_{srm}$  are respectively associated with nonlinear mode-mode interaction of kinetic and available potential energies, and  $D_{srm}$  represents an energy source or sink due to the diabatic process and dissipation. The linear term in (22) does not appear in the energy balance equation because this term does not contribute to the time change of the magnitude of  $w_{srm}$ . Eqs. (33)-(35) should be multiplied by 0.5 for  $s=0$  as in (29). The energetics terms of gravity modes for  $s=0$  were multiplied by 0.5 in this study because a set of Hough vector functions associated with positive and negative eigenfrequencies are the complex conjugate of each other (refer to Kasahara, 1978).

By means of the inverse transforms of the vertical and Fourier-Hough transforms, it can be shown that the summations of all nonlinear mode-mode interactions,  $B_{srm}$  and  $C_{srm}$ , are zero because they represent global integrals of the flux convergences of the kinetic and the available potential energies, respectively:

$$\begin{aligned} & \sum_{s=0}^{\infty} \sum_{r=0}^{\infty} \sum_{m=0}^{\infty} B_{srm} \\ &= \frac{1}{gS} \int_S \int_0^{p_s} [-\nabla \cdot KV - \frac{\partial K\omega}{\partial p}] dp dS = 0, \end{aligned} \quad (36)$$

$$\begin{aligned} & \sum_{s=0}^{\infty} \sum_{r=0}^{\infty} \sum_{m=0}^{\infty} C_{srm} \\ &= \frac{1}{gS} \int_S \int_0^{p_s} [-\nabla \cdot AV - \frac{\partial A\omega}{\partial p}] dp dS = 0. \end{aligned} \quad (37)$$

The vertical change of  $\gamma$  is assumed to be negligible, and the vertical geopotential flux is also assumed to be negligible for the surface integral at  $p_s$ , so as to obtain the relation (37). The second term in (23) represents the vertical geopotential flux at the lower surface. This term has been considered in this study as the secondary importance for the global energetics analysis.

The Hough vector functions are truncated at 26 Rossby modes ( $l_R = 0-25$ ) and 12 gravity modes ( $l_W = 0-11$ ,  $l_E = 0-11$ ). Energetics terms are computed for each observation time and averaged during the data period.

#### 4. Energy Distributions

A summation of energies for all the normal modes is equivalent to the energy integrated over the entire mass of the atmosphere as was discussed before. If we take a summation of energies for all meridional and vertical modes, the resultant energy becomes a function only of the zonal wavenumber. Because both Rossby and gravity modes are involved in Hough harmonics, the energy spectra of those two modes are presented separately.

The distributions of kinetic and available potential energies for Rossby and gravity modes are illustrated in Fig. 2 as a function of zonal wavenumber. The meridional components of the kinetic energy for the Rossby modes are also illustrated in the figure. The kinetic energy spectrum for the Rossby modes follows approximately the -3 power law for  $s > 7$  (Leith, 1971). The available potential energy spectrum also follows the -3 power law (Chen and Wiin-Nielsen, 1978). This range is regarded as an inertial subrange for two dimensional isotropic turbulence in the atmosphere. The kinetic energy level is lower than that expected by the -3 power law for  $s = 1$  to 6. This deflection of the energy distribution is attributable to the meridional component of the kinetic energy. These results are consistent with previous research (e.g.,

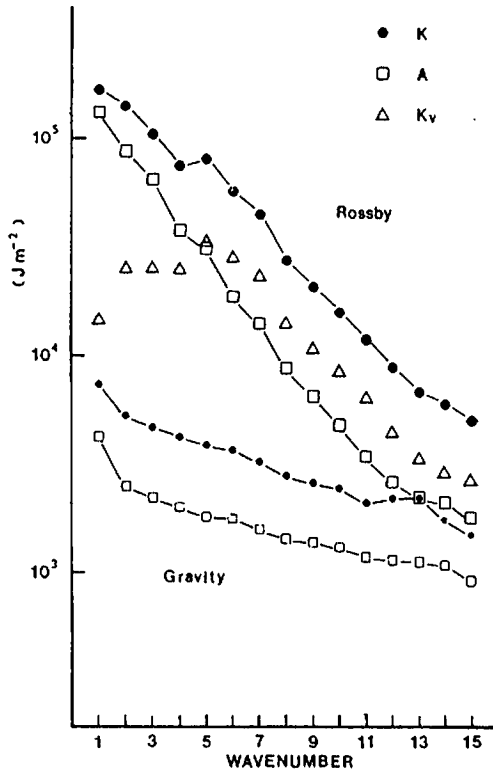


Fig. 2. Energy distributions in the wavenumber domain.  $K$ : kinetic energy,  $A$ : available potential energy,  $K_v$ :  $v$ -component of  $K$

Wiin-Nielsen, 1967). The energy distributions for the gravity modes follow the  $-5/3$  power law, which is also the characteristics of two-dimensional isotropic turbulence in the atmosphere.

Synthesizing the energies with respect to all the zonal wavenumbers and meridional indices for Rossby and gravity modes separately, we obtain the energy spectra in the vertical wavenumber domain. Fig. 3 illustrates the energy distributions of eddy kinetic and eddy available potential energies ( $s = 1-15$ ) for Rossby and gravity modes, respectively. The features are the same for  $s=0$  (not shown). In this study the normal modes for  $s=0$  are obtained according to Kasahara (1978). A large amount of kinetic energy of the Rossby mode is included in the barotropic mode ( $m=0$ ). Another energy peak is seen at  $m=4$  which

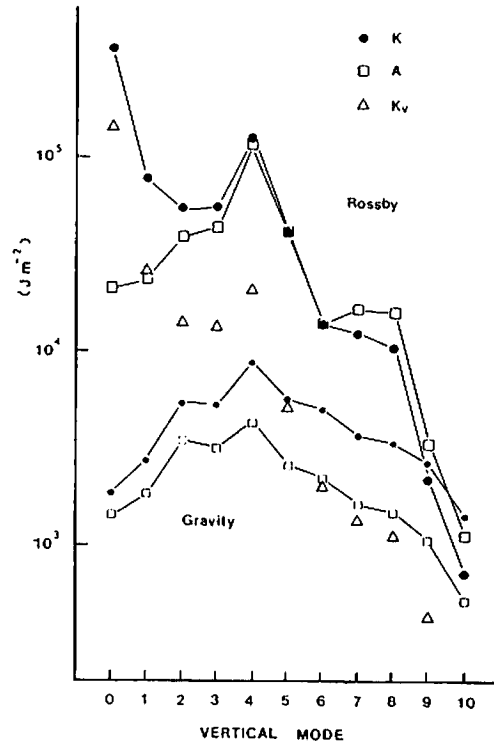


Fig. 3. Eddy energy distributions in the vertical mode domain.

is one of the baroclinic modes. As is seen in Fig. 1, the eigenvector for  $m=4$  has a node near 600 hPa and maximum near 250 hPa. The tropospheric jet near 250 hPa level may cause the secondary maximum of kinetic energy at  $m=4$ . This secondary peak was found at  $m=3$  according to Kasahara and Puri (1981). The distribution of available potential energy for the Rossby mode shows an energy maximum at  $m=4$ . Small temperature deviations from the global mean near 250 hPa may be reflected at  $m=4$ . The reservoir of available potential energy is small (but not zero) for the barotropic mode. The energy reservoir of this mode should vanish if the vertical eigenvector  $m=0$  were exactly constant with respect to pressure. The distribution of both the kinetic and available potential energies for the gravity modes indicate their energy peaks at  $m=4$ .

This result differs from that obtained by Puri (1983) who obtained the energy maximum at  $m=0$  in his model analysis.

The kinetic energy spectra in the meridional wavenumber domain are illustrated in Fig. 4 for  $s=1$  through 6. With the results in Fig. 3, the distributions are presented for  $m=0$  and  $m=4$ . The kinetic energy spectrum for  $s=0$  (not shown) indicates the energy peaks at the first two symmetric modes of the barotropic mode. These two symmetric modes,  $l_R=1$  ( $3.3 \times 10^6 \text{ Jm}^{-2}$ ) and  $l_R=3$  ( $1.9 \times 10^6 \text{ Jm}^{-2}$ ), contain about 50% of the kinetic energy for  $s=0$ . The distribution of available potential energy for  $s=0$  shows an energy peak at the first symmetric mode of  $m=4$ . This single mode,  $l_R=1$  ( $22.7 \times 10^5 \text{ Jm}^{-2}$ ) contains about 50% of the available potential energy of  $s=0$ . The kinetic energy distribution for the Rossby modes of  $s=1$ ,  $m=0$  shows the energy peaks at  $l_R=4$  and 6. The distribution approximately follows the -3 power of the meridional mode number at the range of large meridional modes. A similar result was found by Kasahara and Puri (1981). There is an apparent cut-off of energy at the range of  $l_R < 4$ . It is discussed in Tanaka (1984) that for  $s=1$ ,  $m=0$ , a transition of energy peaks was observed during January 1979 from  $l_R=8$  via 6 to 4. The wave energy started to propagate vertically when the energy peak reached  $l_R=4$  or 3 which is the critical meridional scale for the vertical propagation (see Dickinson, 1968). It is found by the intermediate results of the present study that the energy of  $m=0$  is transformed to  $m=1$  while the vertical propagation occurred. For this results, the meridional index with the energy peak is considered as the critical meridional scale for the vertical propagation of wave energy. The range where the -3 power law is applicable is regarded as pertaining to trapped mode. Conversely the range of smallest meridional index represents the propagative mode. The energy peaks are seen at  $l_R=3$  for  $s=2, 3, 5$  and at  $l_R=2$  for  $s=6$ .

The kinetic energy spectra for  $m=4$  show energy peaks at  $l_R=6, 7$  for  $s=5$  and 6. These energy peaks are associated with the characteristic meridional scale of the cyclone-scale waves. The energy peaks for  $m=4$  are flattened in  $s=1$  or  $s=2$ . The energy spectra for the gravity modes approximately follow the -5/3 power of the meridional mode. The energy level for  $m=0$  tends to decrease as the wavenumber increases, but it remains unchanged for  $m=4$ .

A Hough function is associated with an eigenfrequency which is determined by the horizontal scale of the wave. Using the eigenfrequency as a coordinate, we can investigate the energy spectra in the frequency domain. In Fig. 5 the kinetic energy distribution of barotropic mode is plotted as a function of dimensionless frequency  $\sigma$ . The westward propagating Rossby modes (large symbols) and gravity modes (small symbols) are plotted in the left half of the figure, whereas the small symbols in the right half indicate the eastward propagating gravity modes. Since the energy levels of the gravity modes are low and are accommodated with high frequencies, the energy distributions for the gravity modes are positioned in the lower left and lower right corners of the figure. The distributions show clear energy peaks at the frequency (period)  $\sigma=0.03$  (16 day) for  $s=1$ , and  $\sigma=0.07$  (7day) for  $s=6$ . The energy peak is a function of the wavenumber. These energy maxima correspond to those in the meridional mode domain (Fig. 4). As was discussed previously, the frequency for which the energy peak is observed, corresponds to the critical meridional scale for the vertical propagation. The energy spectra follow approximately the 3 power of the frequency at the low frequency range. On the other hand, the spectrum follows approximately the -5/3 power at the high frequency range of the gravity modes. As is seen in Fig. 2 and 4, the energy spectra of the gravity modes seem to follow the -5/3

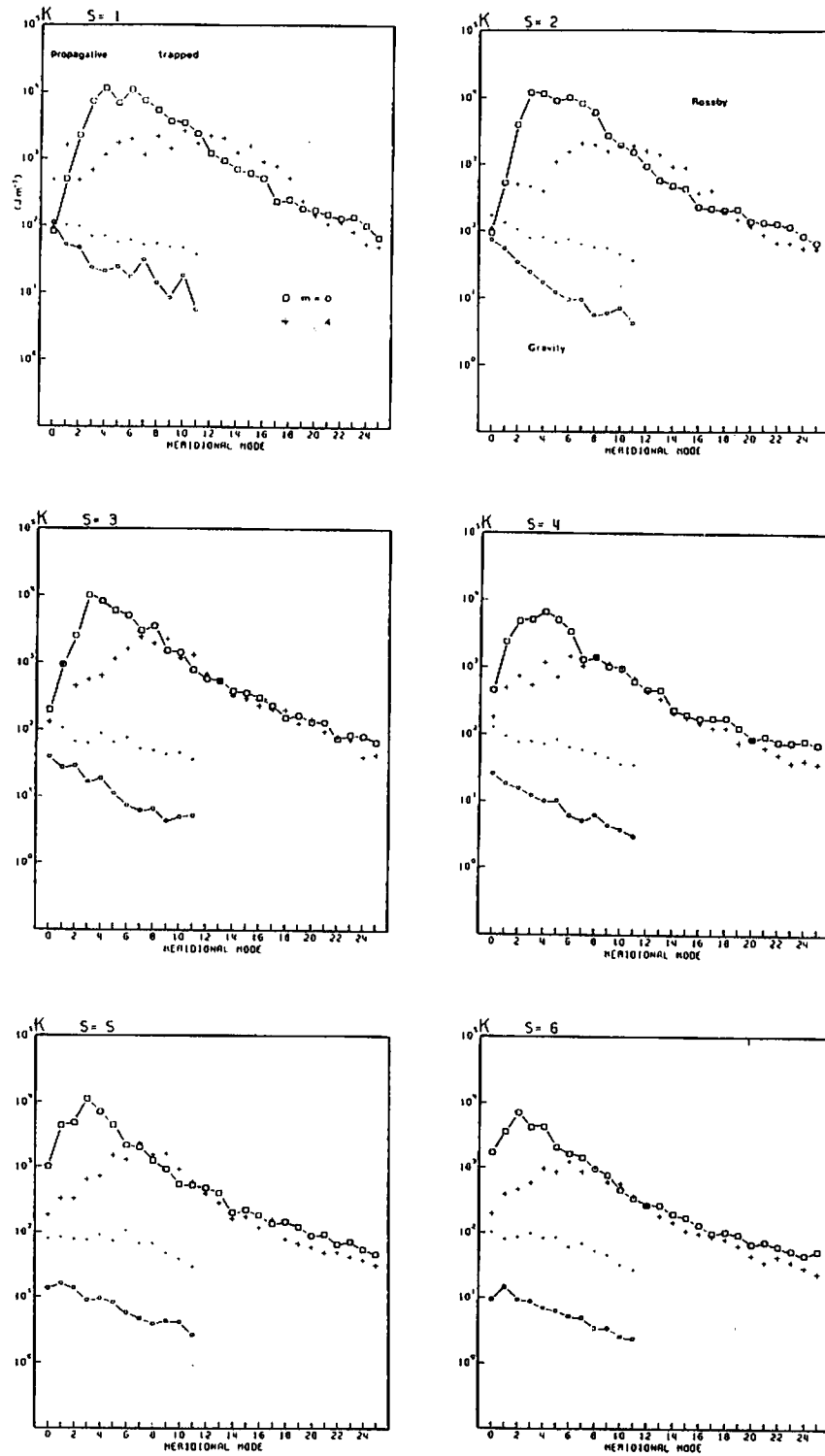


Fig. 4. Kinetic energy distributions in the meridional mode domain for vertical modes  $m=0$  and 4 for the wavenumber  $s=1$  through 6.

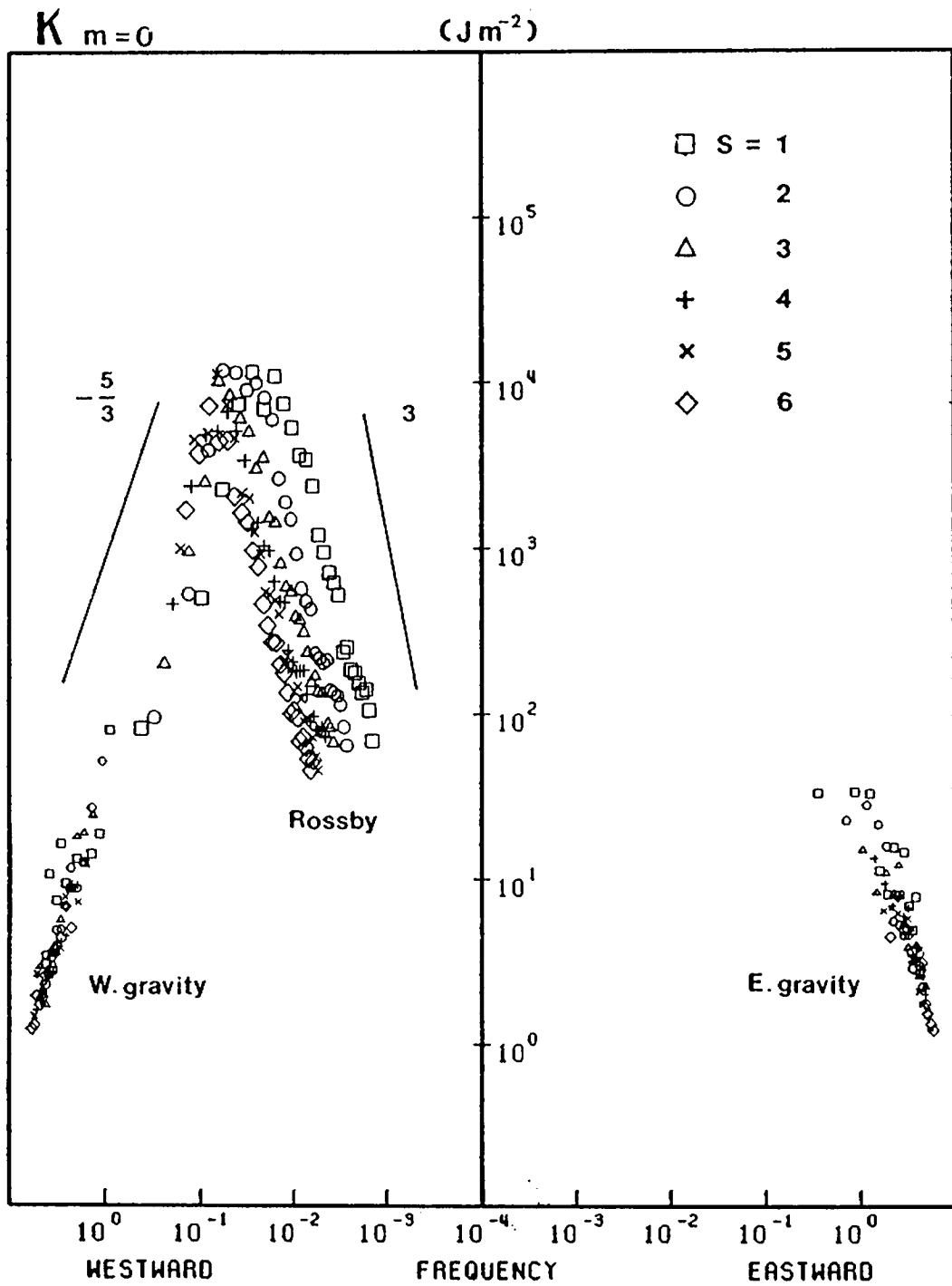


Fig. 5. Kinetic energy distributions in the dimensionless frequency domain for barotropic mode ( $m=0$ ).

power of the zonal wavenumber and meridional index. Because the phase velocity of the gravity mode is a function of the depth of the fluid (equivalent height), and taking into account the relation  $c = \sigma/s$ , we thus have an analogy with the  $-5/3$  power law for the frequency domain. By using the dispersion relationship of the Rossby-Haurwitz waves, the same argument gives us an analogy of the 3 power law for the low frequency range. The most interesting features of this result are that the energy distribution of the largest-scale Rossby modes not only seems to follow the  $-5/3$  power law, but also merges continuously with the distribution of the gravity mode. The mixed Rossby-gravity modes are positioned between the two types of modes. The frequency in the abscissa is determined by the theory for free waves in the motionless atmosphere. Nevertheless, the energy peaks in the frequency domain may be significantly related with forced and free stationary waves in the westerlies. Supposing that the energy peaks correspond to the stationary waves, the spectral distribution turns out to be similar to

that found in previous research concerning the space-time spectra of progressive and retrogressive waves (e.g., Hayashi, 1982). It is conjectured that the meridional scales of the waves are adjusted so that the energy spectra follow the 3 or the  $-5/3$  power law in the motionless atmosphere.

Fig.6 shows the energy distributions of the kinetic energy of  $m=0$  and 4 and the available potential energy of  $m=4$  for the westward propagating Rossby modes as a function of the dimensionless phase velocity ( $c = \sigma/s$ ). It may be readily noted that the distributions of kinetic energy follow approximately the 3 power of the phase velocity independently of the wavenumber. The distribution of available potential energy seems to obey the 5 power law (see Merilees and Warn, 1972).

Before leaving this section, the energy distributions are shown for Kelvin modes and mixed Rossby-gravity modes. Fig. 7(a) illustrates the energy distributions for these modes as a function of wavenumber by summing all the contributions relative to the vertical modes. Most of the energy is included

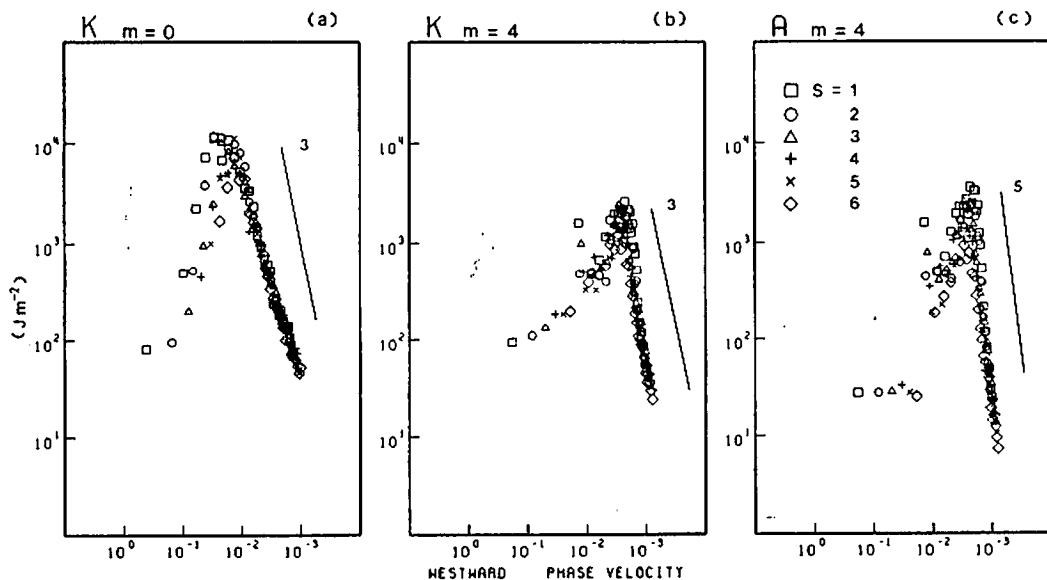


Fig. 6. Energy distributions in the dimensionless phase velocity domain for kinetic energy (a)  $m=0$ , (b)  $m=4$  and for available potential energy (c)  $m=4$ .

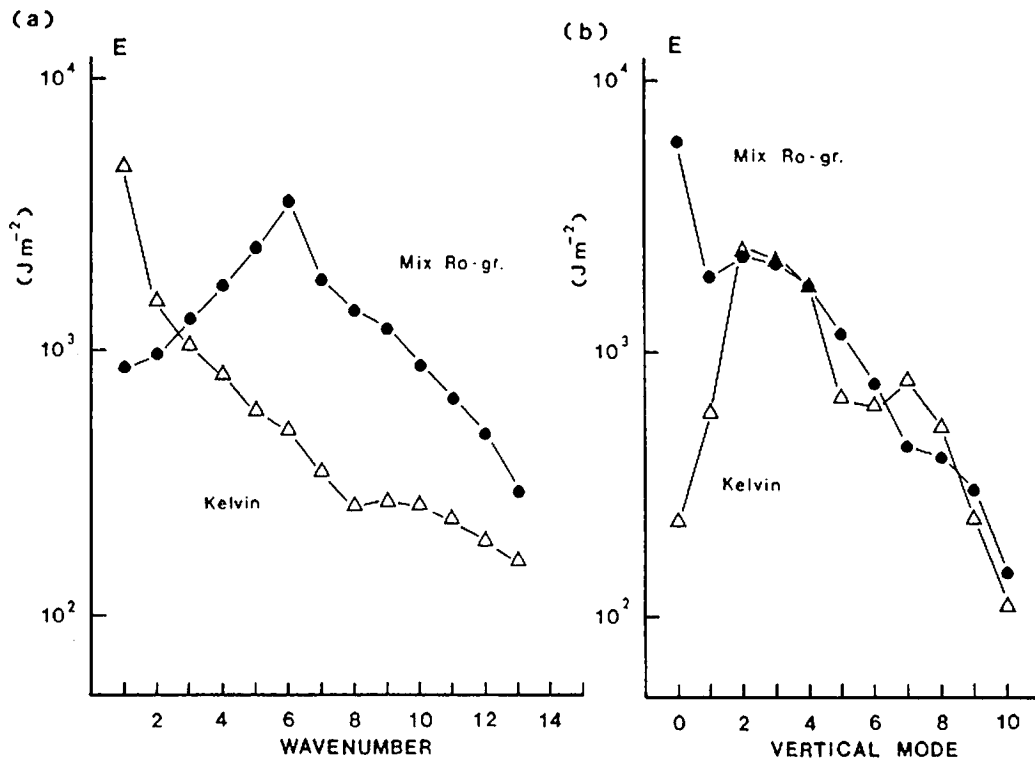


Fig. 7. Energy distributions for Kelvin and mixed Rossby-gravity modes in the (a) wavenumber domain and (b) vertical mode domain.

in the planetary waves for the Kelvin modes, whereas the mixed Rossby-gravity modes indicate an energy peak in the cyclone-scale waves. Fig. 7(b) illustrates the energy distributions as a function of vertical mode obtained by a summation over all the wavenumbers. Most of the energy is included in the barotropic mode for the mixed Rossby-gravity modes. The Kelvin modes show an energy maximum in the range of  $m=2$  to 4, and the energy level is very low at the barotropic mode.

**5. Energy Interactions**

We start the examination of the energy interactions in the wavenumber domain by synthesizing all the vertical and meridional modes. The results for all the vertical modes ( $m=0-11$ ) are illustrated in Fig. 8(a). Fig. 8(b) and (c) show the separation into barotropic ( $m$

$= 0$ ) and baroclinic modes ( $m = 1-11$ ), respectively. The results are presented only for the Rossby modes excluding the gravity modes unless otherwise mentioned. The distribution for  $m=0-11$  is equivalent to Fig. 1 in Kung and Tanaka (1984). The term  $C$  corresponds to  $R(n) + S(n)$  and the term  $B$  to  $M(n) + L(n)$  in the mentioned paper except that these results are for the Rossby mode only.

The positive value of the nonlinear interaction  $C$  means that the zonal available potential energy is transformed into the eddy available potential energy. By means of separation of this interaction into the barotropic and the baroclinic modes, it is found that most of the interaction is included in the barotropic mode. In particular, the wavenumber 2 show large interaction. The interaction by the baroclinic mode is small for all the wavenumbers. However, this result is

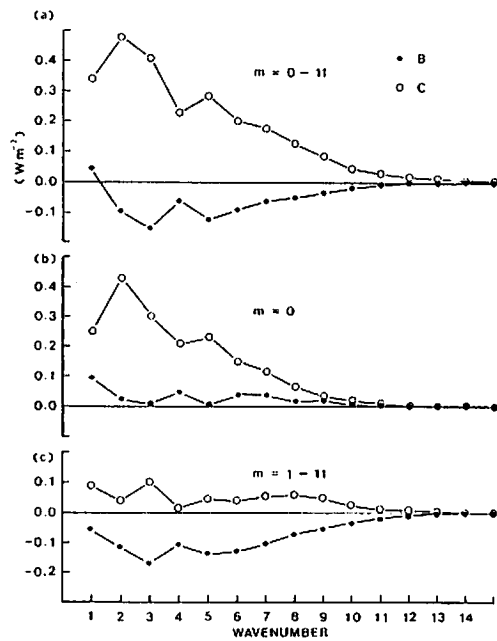


Fig. 8. Energy interactions in the wavenumber domain for (a)  $m=0-11$ , (b)  $m=0$  and (c)  $m=1-11$  B : Interactions of kinetic energy (Rossby mode), C : those of available potential energy.

modified in Tanaka and Kung (1988) by assuming the vanishing wind at the lower surface. This assumption should be physically correct due to the surface friction, and the vanishing heat advection at the lower surface in (12) appears to reduce the barotropic component of the term C. The increased C at the baroclinic components can balance with the negative value of B. This interpretation of the atmospheric energy flow is physically reasonable. Hence, the result described by Tanaka and Kung (1988) would represent the real energy flow, and the result illustrated in this Fig. 8 can be incorrect. It is found in this study that the analysis result is extremely sensitive to the treatment of the lower surface wind.

On the other hand, the nonlinear interaction for the kinetic energy, B, for  $m=0-11$  shows negative values. This means that the eddy kinetic energy is transformed into the zonal kinetic energy. The separation of the

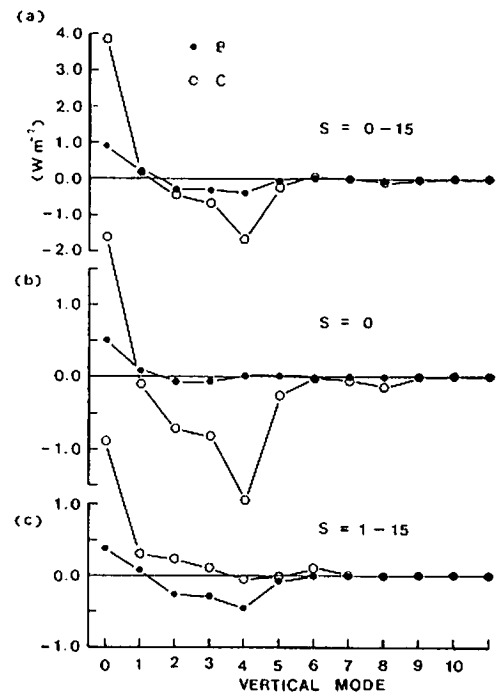


Fig. 9. Energy interactions (Rossby mode) in the vertical mode domain for (a)  $s=0-15$ , (b)  $s=0$  and (c)  $s=1-15$ .

interaction into the barotropic and the baroclinic modes reveals that these features are valid only for the baroclinic mode. On the contrary, the direction of the energy flow for the barotropic mode is opposite to that for the baroclinic mode. This result would be important for an investigation of barotropic instability because the result suggests the possibility of an energy flow from the zonal kinetic energy to the eddy kinetic energy in a climatological sense. Nevertheless, the kinetic energy of the barotropic mode seems to be supplied by the baroclinic modes instead of by the zonal motions as will be shown later.

Fig. 9 illustrates the distributions of the nonlinear interaction in the vertical mode domain for all wavenumbers ( $s=0-15$ ), zonal ( $s=0$ ) and eddy ( $s=1-15$ ) obtained by a similar procedure as in Fig. 8. The available potential energy generated in the zonal baroclinic mode, especially  $m=4$ , is transformed into both the



zonal and eddy available potential energies of the barotropic mode. Similarly the kinetic energy is transformed from the baroclinic mode to the barotropic mode. Evidently, the kinetic energy of the barotropic mode is supplied by the baroclinic mode. The nonlinear interactions for the available potential energy and the kinetic energy are visibly expressed in Fig. 10, where the abscissa corresponds to zonal wavenumber and the ordinate to the vertical index. The arrow in Fig. 10(a) indicates the energy flow of the available potential energy from the zonal baroclinic

mode to the planetary scale barotropic mode. If we assume the vanishing lower surface wind as discussed above, however, the result will show the energy flow from zonal baroclinic components to eddy baroclinic components. Likewise, the arrows in Fig. 10(b) indicate the energy flow of the kinetic energy from the eddy baroclinic mode to the zonal and eddy barotropic modes. Zonal kinetic energy is supplied by the eddy kinetic energy of the baroclinic mode.

Finally, the normal mode energetic variable are summarized in Table 2 in terms of the

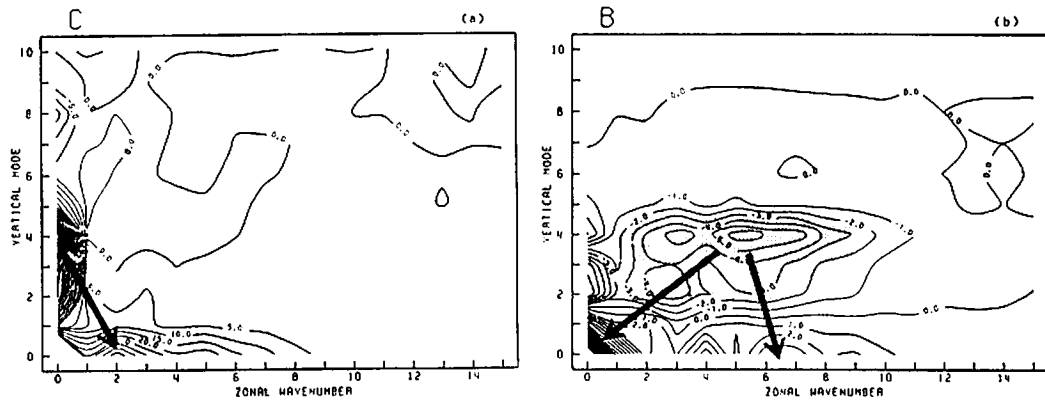


Fig.10. Energy interactions (Rossby mode) in the wavenumber and vertical mode domains for (a) available potential energy and for (b) kinetic energy. Large negative values (energy outflow) are hatched. Unit :  $10^{-2} \text{ Wm}^{-2}$ .

Table 2. Energy balance for the classified modes in the wavenumber, vertical mode and meridional mode domains. Units are  $10^5 \text{ Jm}^{-2}$  for energy,  $\text{Wm}^{-2}$  for interactions.

mode	$K_z$	$K_e$	$K$	$A$	$E$	$B$	$C$	$B+C$
$s=0$	10.6	0.0	10.7	50.5	61.2	0.39	-1.93	-1.54
$s=1-5$	4.6	1.4	5.9	3.7	9.6	-0.38	1.73	1.35
$s=6-10$	0.9	0.9	1.8	0.6	2.4	-0.25	0.60	0.36
$s=11-15$	0.2	0.2	0.5	0.2	0.7	0.01	0.07	0.08
$m=0$	8.6	1.5	10.1	2.1	12.2	0.78	3.86	4.64
$m=1-11$	7.7	1.1	8.9	52.8	61.7	-1.00	-3.39	-4.39
Rosby	16.1	2.3	18.4	51.7	73.1	-0.21	0.44	0.23
West-gr.	0.1	0.2	0.3	0.1	0.4	0.02	-0.02	-0.01
East-gr.	0.1	0.1	0.3	0.2	0.4	-0.03	0.05	0.03
Sym.	12.5	1.3	13.7	48.5	62.2	0.07	-0.52	-0.44
Antisym.	3.9	1.3	5.2	6.5	11.7	-0.29	0.99	0.70

classified modes in the wavenumber vertical mode and meridional mode domains. The zonal and eddy energy levels are respectively 10.7 and 8.2 ( $10^{11} \text{ Jm}^{-2}$ ) for the kinetic energy and 50.5 and 4.5 ( $10^{11} \text{ Jm}^{-2}$ ) for the available potential energy. These values agree reasonably well with previous results (Kung and Tanaka, 1983) despite the fact that the kinetic and available potential energies have been retrieved by the total energy through multiplication by the coefficients  $\beta_w$ ,  $\beta_v$ ,  $\beta_z$ . The energy interactions between zonal and eddy kinetic energies and between zonal and eddy available potential energies are 0.39 and -1.93 ( $\text{Wm}^{-2}$ ), respectively. These energy interactions are also reasonably close to those found in previous research notwithstanding the fact that the period of analysis is slightly longer in this study and the stability parameter for the available potential energy is fixed by the annual mean state. Decompositions of the energy and energy interactions into the barotropic and the baroclinic modes reveal that a large amount of energy is transformed from the baroclinic mode to the barotropic mode. This indicates that the energy is generated in the baroclinic mode and dissipated in the barotropic mode. This energy flow is reasonable because large amount of available

potential energy ( $s = 0$ ) is converted to eddy kinetic energy in the atmosphere, where the former must be included in the baroclinic mode but the latter is dominated in the barotropic mode. Decompositions into the Rossby mode and the westward and eastward gravity modes show that the energy of the gravity modes is about 1% of that of the Rossby mode for the case of the GFDL version of the FGGE data. Decompositions into the symmetric and antisymmetric modes show that 75% of the energy is included in the symmetric mode and 15% in the antisymmetric mode. Although, as a total, the energy is transformed from the symmetric to the antisymmetric mode, the kinetic energy interactions indicate a reverse energy flow from the antisymmetric to the symmetric mode.

The same energetic variables are listed in Table 3 for the Kelvin mode, the mixed Rossby-gravity mode and several low-order Hough modes which appeared in the recent papers. The values for the Kelvin and the mixed Rossby-gravity modes are obtained by the summation over all wavenumbers and vertical modes. The numbers in the parentheses for these single Hough modes denote wavenumber  $s$ , meridional mode  $l_R$  and

Table 3. Energy balance for Kelvin, mixed Rossby-gravity modes and low-order Hough modes ( $s, r, m$ ). Units are  $10^{11} \text{ Jm}^{-2}$  for energy, and  $10^{-2} \text{ Wm}^{-2}$  for interactions.

mode	$K_e$	$K_v$	$K$	$A$	$E$	$B$	$C$	$B+C$
Kelvin	5.4	0.0	5.4	5.7	11.1	1.5	0.4	1.8
Mix Ro-gr.	1.9	14.2	16.1	1.4	17.5	-1.4	1.5	0.1
(1,1,0)	0.4	0.1	0.5	0.3	0.8	-0.2	-1.1	-1.3
(1,2,0)	1.7	0.5	2.3	0.9	3.1	-0.1	-4.8	-4.9
(1,3,0)	5.8	1.5	7.3	1.8	9.1	0.7	2.3	3.0
(1,4,0)	9.4	2.0	11.4	1.8	13.3	1.9	2.1	4.0
(2,1,0)	0.3	0.3	0.5	0.1	0.6	-0.2	1.3	1.1
(2,2,0)	2.3	1.6	3.9	0.7	4.6	-1.8	6.9	5.1
(2,3,0)	7.7	4.1	11.7	1.6	13.4	-0.9	6.7	5.8
(3,1,0)	0.3	0.6	0.9	0.1	1.1	-0.2	0.1	-0.1
(3,2,0)	1.2	1.3	2.5	0.3	2.8	0.0	1.5	1.5

vertical mode  $m$ , respectively. The Kelvin mode involves about the same amount of kinetic energy ( $u$ - component) and available potential energy. Both the kinetic and available potential energies gain their energy through the nonlinear interactions. The mixed Rossby-gravity mode has a large part of energy in the meridional component of the kinetic energy. This mode gains available potential energy and loses kinetic energy through the nonlinear interactions. The Hough modes (1,1,0) and (1,3,0) were proposed by Madden (1978) as 5-day waves and 16-day waves, respectively. The former loses energy and the latter gains energy through the nonlinear interactions.

## 6. Summary and Conclusions

The results of the normal mode energetics analysis applied to the GFDL version of the FGGE data during the winter period from December 1978 to February 1979 are summarized as follows:

The energy spectrum in the vertical wavenumber domain for the Rossby mode indicates an available potential energy peak in the vertical wavenumber  $m = 4$ , and a kinetic energy peak in the barotropic component ( $m = 0$ ). The kinetic energy spectrum shows a secondary energy peak at  $m = 4$ . The available potential energy generated at the zonal baroclinic components (especially  $m = 4$ ) is transformed to the eddy available potential energy of barotropic components. This result is, however, modified as to eddy baroclinic components by Tanaka and Kung (1988) by the assumption of vanishing the lower surface wind for the data analysis. On the other hand, the kinetic energy of the cyclone-scale baroclinic mode ( $m = 2-4$ ) is transformed to zonal and eddy kinetic energies of the barotropic mode by nonlinear interactions. Consequently, the atmospheric energy flow is characterized by the energy interaction from baroclinic mode to barotropic mode. Thus,

most of the kinetic energy is dissipated by the barotropic mode.

Parameterizing the horizontal scale of waves by their eigenfrequencies, we find in the frequency domain that the kinetic energy spectra for the barotropic mode indicate clear energy peaks at the frequency  $\sigma = 0.03$  (16 day) for the wavenumber 1 and  $\sigma = 0.07$  (7 day) for the wavenumber 6. The spectral characteristics are distinguished by the 3-D scale of the waves. The energy spectra follow approximately the 3 power of the frequency for the smaller-scale waves in the low frequency range. However, for the largest-scale Rossby modes in the high frequency range, the spectrum obeys the  $-5/3$  power law and merges continuously with the spectrum of the gravity modes. It is concluded from these results that the energy spectrum of the planetary Rossby waves is similar to that of gravity waves for the global scale waves.

## Acknowledgments

The author appreciates Professor E.C. Kung of the University of Missouri-Columbia. Thanks are also due to Dr. A. Kasahara of the National Center for Atmospheric Research for consultation. The author is grateful to Dr. J.A.M. Corte-Real and J.R. Angel for reading the manuscript and J.C. Tseng and S.J. Brooks for the technical assistance.

## References

- Ahlquist, J.F. (1982): Normal-mode global Rossby waves: Theory and observations. *J. Atmos. Sci.*, **39**, 193-202.
- Chen, T.-C. and A. Wilm-Neilsen (1978): On nonlinear cascades of atmospheric energy and enstrophy in a two-dimensional spectral index. *Tellus*, **30**, 313-322.
- Dickinson, R.E. (1968): On the exact and approximate liner theory of vertically propagating planetary Rossby waves forced at a spherical lower boundary. *Mon. Wea. Rev.*, **96**, 405-415.
- Eliassen, E. and B. Machenhauer (1965): A study of the fluctuation of atmospheric planetary flow patterns represented by spherical harmonics. *Tellus*, **17**, 220-238.

- Garcia, R.G. and J.E. Geisler (1981): Stochastic forcing of small amplitude oscillation in the stratosphere. *J. Atmos. Sci.*, **38**, 2187-2197.
- Hayashi, Y. (1980): Estimation of nonlinear energy transfer spectra by the cross-spectral method. *J. Atmos. Sci.*, **37**, 299-307.
- Hayashi, Y. (1982): Space-time spectral analysis and its applications to atmospheric waves. *J. Meteor. Soc. Japan*, **60**, 156-171.
- Hirota, I. (1971): Excitation of planetary Rossby waves in the winter stratosphere by periodic forcing. *J. Meteor. Soc. Japan*, **49**, 439-449.
- Holmstrom, I. (1963): On a method for parametric representation of the state of the atmosphere. *Tellus*, **15**, 127-149.
- Holton, J. R. (1975): *The dynamic meteorology of the stratosphere and mesosphere*. Meteor. Monogr., No. 37, Amer. Meteor. Soc., 218pp.
- Kao, S.-K. (1968): Governing equations and spectra for atmospheric motion and transports in frequency wavenumber space. *J. Atmos. Sci.*, **25**, 32-38.
- Kasahara, A. (1976): Normal modes of ultralong waves in the atmosphere. *Mon. Wea. Rev.*, **104**, 669-690.
- Kasahara, A. (1978): Further studies on a spectral model of the global barotropic primitive equations with Hough harmonic expansions. *J. Atmos. Sci.*, **35**, 2043-2051.
- Kasahara, A. (1980): Effect of zonal flows on the free oscillations of a barotropic atmosphere. *J. Atmos. Sci.*, **37**, 917-929.
- Kasahara, A. (1984): The linear response of a stratified global atmosphere to tropical thermal forcing. *J. Atmos. Sci.*, **41**, 2217-2237.
- Kasahara, A. and K. Puri (1981): Spectral representation of three dimensional global data by expansion in normal mode functions. *Mon. Wea. Rev.*, **109**, 37-51.
- Kung, E.C. and H. Tanaka (1983): Energetics analysis of the global circulation during the special observation periods of FGGE. *J. Atmos. Sci.*, **40**, 2575-2592.
- Kung, E.C. and H. Tanaka (1984): Spectral characteristics and meridional variations of energy transformations during the first and second special observation periods of FGGE. *J. Atmos. Sci.*, **41**, 1836-1849.
- Leith, C.E. (1971): Atmospheric predictability and two-dimensional turbulence. *J. Atmos. Sci.*, **28**, 145-161.
- Lindzen, R.S., D.M. Straus and B. Katz (1984): An observational study of large-scale atmospheric Rossby waves during FGGE. *J. Atmos. Sci.*, **41**, 1320-1335.
- Longuet-Higgins, M.S. (1968): The eigenfunction of Laplace's tidal equation over a sphere. *Phil. Trans. Roy. Soc., London*, **A262**, 511-607.
- Lorenz, E.N. (1955): Available potential energy and the maintenance of the general circulation. *Tellus*, **7**, 157-167.
- Madden, R. (1978): Further evidence of traveling planetary waves. *J. Atmos. Sci.*, **35**, 1605-1618.
- Merilees, P.E. and Warn, T. (1972): The resolution implications of geostrophic turbulence. *J. Atmos. Sci.*, **29**, 990-991.
- Miyakoda, K., J. Sheldon and J. Sirutis (1982): Four-dimensional analysis experiment during the GATE period. *Part II. J. Atmos. Sci.*, **39**, 4896-506.
- Puri, K. (1983): The relationship between convective adjustment, Hadley circulation, and normal mode of the ANMRC spectral model. *Mon. Wea. Rev.*, **111**, 23-33.
- Salby, M. (1981): Rossby normal modes in nonuniform background configurations. Part II: Equinox and solstice conditions. *J. Atmos. Sci.*, **38**, 1827-1840.
- Saltzman, B. (1957): Equations governing the energetics of the larger scales of atmospheric turbulence in the domain of wavenumber. *J. of Meteorology*, **14**, 513-523.
- Tanaka, H.L. (1984): On the amplification and vertical propagation of zonal wavenumber 1 for January 1979. *Gross Wetter*, **22**, No. 2, 17-25., (in Japanese).
- Tanaka, H.L. and E.C. Kung (1988): Normal mode energetics of the general circulation during the FGGE year. *J. Atmos. Sci.*, **45**, 3723-3736.
- Wiin-Nielsen, A. (1967): On the annual variation and spectral distribution of atmospheric energy. *Tellus*, **19**, 540-559.

**APPENDIX: List of Symbols**

$\lambda$	: longitude	$h_m$	: equivalent height
$\theta$	: latitude	$G_m$	: vertical eigenvector
$p$	: pressure	$\alpha_m$	: dimensionless parameter in Eq. (15)
$t$	: time	$E$	: total energy $A + K$ .
$u$	: zonal	$A$	: available potential energy
$v$	: meridional velocity	$K$	: kinetic energy $K_u + K_v$ .
$\omega$	: vertical p-velocity	$K_u$	: kinetic energy of u-component
$T$	: perturbation temperature	$K_v$	: kinetic energy of v-component
$\phi$	: perturbation geopotential	$\beta$	: energy ratio of Hough function $\beta_u + \beta_v + \beta_z = 1$
$F_u$	: frictional force in zonal direction	$\sigma_{sm}$	: eigenfrequency
$F_v$	: frictional force in meridional direction	$H_{sm}$	: Hough harmonics
$Q$	: diabatic heat source	$\Theta_{sm}$	: Hough vector function
$a$	: radius of the earth	$W_m$	: dimensionless variable vector
$g$	: gravity of the earth	$B_m$	: dimensionless nonlinear term vector for wind field
$\Omega$	: angular velocity of the earth's rotation	$C_m$	: dimensionless nonlinear term vector for mass field
$R$	: specific gas constant	$D_m$	: dimensionless vector of friction and diabatic heating
$C_p$	: specific heat at constant pressure	$w_{sm}$	: Fourier-Hough transform of $W_m$
$p_s$	: surface pressure of basic state	$b_{sm}$	: Fourier-Hough transform of $B_m$
$T_s$	: surface temperature of basic state	$c_{sm}$	: Fourier-Hough transform of $C_m$
$T_0$	: temperature of basic state	$d_{sm}$	: Fourier-Hough transform of $D_m$
$\gamma$	: stability parameter in Eq. (4)	$B_{sm}$	: nonlinear mode-mode interaction of kinetic energy
$S$	: whole area of isobaric surface	$C_{sm}$	: nonlinear mode-mode interaction of available potential energy
$s$	: zonal wavenumber	$D_{sm}$	: energy source and sink
$r$	: meridional mode		
$m$	: vertical mode		
$l_R$	: meridional mode for Rossby mode		
$l_W$	: meridional mode for westward gravity mode		
$l_E$	: meridional mode for eastward gravity mode		



---

